

Stability of monatomic and diatomic quasicrystals and the influence of noise

J. Roth

*Institut für Theoretische und Angewandte Physik der Universität Stuttgart, Pfaffenwaldring 57,
D-7000 Stuttgart 80, Federal Republic of Germany*

R. Schilling

Institut für Physik, Universität Basel, Klingelbergstrasse 82, CH-4056 Basel, Switzerland

H.-R. Trebin

*Institut für Theoretische und Angewandte Physik der Universität Stuttgart, Pfaffenwaldring 57,
D-7000 Stuttgart 80, Federal Republic of Germany*

(Received 30 March 1989; revised manuscript received 6 September 1989)

The stability of quasicrystals endowed with atomic Lennard-Jones-like pair potentials was investigated with use of the method of steepest descent. Starting from two- and three-dimensional Penrose patterns, the basic units were decorated in various fashions with one or two sorts of atoms. In accord with previous studies, all monatomic two-dimensional quasicrystals decay to a hexagonal periodic crystal with defects; diatomic systems remain stable when the relative size of the atoms is suitably chosen. In three dimensions, the monatomic quasicrystalline unit-sphere packing was proven stable as well as the structure of truncated icosahedra, even if in the initial configuration the atoms were displaced statistically up to 7% and 25%, respectively, of the edge length (noise). A series of decorations (among them one involving Mackay icosahedra) relaxed to the amorphous state. In these transitions the atoms arrange in families of Fibonacci planes whose separations scale down to atomic distances in a self-similar fashion.

I. INTRODUCTION

Solid matter can occur as different types of structures. These are periodic (crystals), quasiperiodic (conventional incommensurate structures), aperiodic (glasses), and as we have known since 1984, quasicrystalline structures. The crucial property of quasicrystals which makes them so different from the conventional incommensurate structures is the combination of noncrystallographic symmetry and sharp diffraction peaks.

To prove the existence and stability of these structures from a microscopic point of view is rather hard for both the conventional structures as well as for the quasicrystals. Concerning quasicrystals, one of the first approaches has been a phenomenological one using a Landau-type theory.¹⁻⁶ There the free-energy is expanded in powers of $\rho(\mathbf{q})$, the Fourier components of the mass density, with wave vectors \mathbf{q} pointing, e.g., along the edges of an icosahedron. It is found that stability may exist. Microscopic models were used by several authors. Let us first mention the work in two dimensions. Lançon *et al.*^{7,8} and Sasajima *et al.*⁹ have performed molecular-dynamics calculations. Starting with a monatomic Penrose pattern and a Lennard-Jones potential it was found in Ref. 9 that the pattern is unstable, relaxing to a hexagonal lattice with some defects. However, decorating the Penrose pattern with two types of particles, Lançon *et al.*^{7,8} confirmed stability (using a Johnson-like potential), provided that the temperature is low enough. A similar result was obtained by Widom *et al.*¹⁰ from Monte Carlo simulations of a two-component Lennard-Jones system and by Leung *et al.*¹¹ for a diatomic dodecagonal quasicrystal. Janssen demonstrated the stability of a very different pentagonal diatomic quasicrystal in a

relaxation model.¹²

Concerning three-dimensional systems, Szeto and Villain¹³ have shown that a densely packed hard-sphere model does not exhibit quasiperiodic solutions for the *ground state*. Burkov and Levitov¹⁴ have proved analytically that under some assumptions the ground state of a d -dimensional tiling with codimension 1 can be quasicrystalline if the interactions between the tiles are reaching far enough. Similar possibilities were discussed by Narasimhan and Jarić.¹⁵ Some speculations about the energies of three-dimensional Lennard-Jones quasicrystals are contained in an article of Levine and Steinhardt.¹⁶ Matching rules¹⁶⁻¹⁸ also imply the possibility of having a quasicrystal ground state of a local Hamiltonian. Recently, Janssen¹² presented a spring model where the atoms in a three-dimensional quasicrystal interact harmonically, and calculated the density of phonon states.

Like Sasajima *et al.*⁹ we have used a Lennard-Jones-like potential. But instead of dealing with molecular dynamics we applied a *steepest-descent* algorithm starting from two- and three-dimensional *one-component* Penrose patterns.¹⁹ In two dimensions the previous results are confirmed, i.e., monatomic systems proved unstable, and decorated diatomic systems were stable. In three dimensions the initial Penrose pattern relaxes to a glassy state if all vertices of the rhombohedra are occupied. If, however, atoms are removed according to the unit-sphere packing discussed by Henley,²⁰ even the *monatomic* quasicrystal remains stable, or more precisely metastable. Thus, our results demonstrate that it is *not* necessary for the stability of three-dimensional quasicrystals to have at least two sorts of atoms.

The purpose of this paper is twofold: first, to give more details of our previous calculations of Ref. 19, and

second, and more important, to extend these calculations. One of these extensions concerns the *degree of metastability* for the metastable monatomic quasicrystals. This point addresses the question of how much the atoms may fluctuate from their positions in the Penrose pattern such that the system still relaxes to a quasicrystalline structure. Using a Gaussian distribution for these fluctuations we have found that the unit-sphere packing still relaxes to a quasicrystal if the mean fluctuation does not exceed a critical value which is about 7% of the edge length of the rhombohedra. For larger values the system turns into an amorphous structure. Diatomic quasicrystals of suitable decoration return to quasicrystalline order even with much higher initial noise.

The second extension is the study of three-dimensional, two-component systems. Depending on the decoration, we obtain both stable and unstable systems. These results, therefore, may be useful for presorting the structure models of binary quasicrystals.

The paper is organized as follows. In Sec. II we present the model for Lennard-Jones systems. The steepest-descent method and the structural analysis are described in Sec. III. A short section (Sec. IV) is devoted to the two-dimensional systems. Section V contains the results for the three-dimensional monatomic model, supplemented in Sec. VI for two-component models. A summary and a discussion of the results will be given in Sec. VII.

II. THE MODEL

The perfect quasicrystalline rhombohedral tiling is constructed by the grid method in two dimensions and also in three dimensions. Initially, all vertices of the rhombs or rhombohedra are covered with atoms. Modifications are made in three dimensions by removing subsets of the vertices, or, what is equivalent due to the scale invariance of the quasicrystals, by inserting subsets of atoms in an inflated quasilattice.

The centers of the atoms are the origins for the pair interaction potential. We use a truncated Lennard-Jones potential of the following form:

$$V_{LJ}(r) = \begin{cases} E \left[\left(\frac{\sigma}{r} \right)^{12} - 2 \left(\frac{\sigma}{r} \right)^6 \right] \cos^2 \left[\frac{\pi}{2} \frac{1}{\beta} \frac{r}{\sigma} \right] & \text{if } 0 < \frac{r}{\sigma} \leq \beta \\ 0 & \text{if } \frac{r}{\sigma} \geq \beta. \end{cases} \quad (1)$$

Here r denotes the distance $|\mathbf{r}_i - \mathbf{r}_j|$ between the atoms i and j , σ the radius of the potential minimum, β a truncation factor (always taken as 2 here) to make the potential range finite, and E sets the energy scale. The truncation of the potential defines a sufficiently small shell of interaction for every atom which is necessary for computation. Using a finite range, the time for calculation grows linearly with the number of atoms; otherwise it would grow with the square.

For diatomic systems we must replace β , σ , and E by β_{ab} , σ_{ab} , and E_{ab} for atoms of types a and b and therefore three different potential types are used.

The radius σ of the potential minimum was optimized before relaxation by fixing the atoms to their initial position and minimizing the total interaction energy. The optimal value of σ is always close to the shortest separation of atoms in the decoration. This minimum separation R_{\min} , however, frequently is smaller than the radius R of the first *pronounced* shell of atoms (having an appreciable occupation number). As a rule, stability was registered if $\sigma \approx R_{\min}$ and $R_{\min} \approx R$. But the system was unstable if $\sigma \approx R_{\min}$ and $R_{\min} < R$, and even when testing several values of σ in the whole range between R_{\min} and R we could not stabilize it, except in trivial cases (see Sec. V).

In two dimensions, no finite-size effects were found; in three dimensions these were appreciable. Therefore we had to use periodic boundary conditions, which we implemented by rational approximants in the following way. To construct a Penrose tiling we used the grid formalism. The six-dimensional points in the strip which are to be projected into three dimensions can be found easily by dualizing the cells of the grid. We replaced the usually rational independent grid vectors by rational dependent ones, but left the tiling vectors unchanged. The same procedure is found in Refs. 21 and 22, where the orientation of the strip is changed to a rational direction, but the projection direction remains irrational.

In the approximated case the grid vectors are $(p, q, 0)$, $(p, -q, 0)$, $(q, 0, p)$, $(0, p, q)$, $(0, p, -q)$, and $(q, 0, -p)$, where p and q are integers of the Fibonacci chain. In the perfect grid, the grid vectors point to the vertices of an icosahedron and span an irrational grid, but for $p/q = 1/0$ and $1/1$ we get a simple cubic and a centered cubic grid, respectively. Higher approximations only yield tetrahedral symmetry T_h (which includes reflections on the x - y , y - z , and z - x planes) of the grid planes. The grid vectors (of equal length) produce an approximated tiling with a cubic cell of periodicity. The possible range of the approximants p/q of τ is $2/1$, $3/2$, and $5/3$, yielding a periodicity length $2(\tau p + q)(\tau + 2)^{-1/2}$.

The rational approximation yields a different frequency of the possible vertex types but does not alter the local geometry of the tiling pattern.

III. THE METHOD

We have used numerical computation to study the stability of the quasicrystals and analytical tools to examine structure and temporal changes. The basic features of the relaxation procedure and analysis will be described in the following sections.

A. Relaxation

Although the method of "steepest descent" is static, it can, however, be interpreted dynamically as describing an overdamped atomic motion at zero temperature. In a first step we calculate the force

$$\mathbf{F}_i(\mathbf{x}_i) = -\frac{\partial V}{\partial \mathbf{x}_i} = -\sum_{\substack{j=1 \\ (j \neq i)}}^N \frac{\partial V_{\text{LJ}}(\mathbf{r}_{ij})}{\partial \mathbf{r}_{ij}}$$

where $\mathbf{r}_{ij} = |\mathbf{x}_i - \mathbf{x}_j|$ (2)

which atom i feels from all atoms j in its own potential range. Then each atom is displaced by a vector $\delta_i = \lambda \mathbf{F}_i$. Through normalizing δ_i by the maximal force $\max |\mathbf{F}_k|$ we ensure that the largest displacement is λ . The procedure is iterated until equilibrium (minimal energy) is obtained. We used the relative change $\Delta E/E$ of the energy per atom to decide whether the atoms have reached the final state. When the pattern is near the minimum of the energy, overrelaxation can happen if the displacement vectors δ_i are too large, and then the energy increases again. To avoid overrelaxation the steps are diminished by dividing the displacement parameter λ by 2. The number of iterations ranges from 100 to 1000. In most cases we stopped relaxation, when the relative change of energy $\Delta E/E$ per iteration was less than the numeric precision. Relaxation for unstable open clusters was the slowest. Here we stopped at $\Delta E/E = 10^{-5}$.

In 1983 Mercier and Levy²³ used a similar method to examine the stability of "amorphous" clusters with icosahedral symmetry; at present we would call them quasicrystalline.

B. Structural analysis

The straightforward way to examine a structure is by depicting it in real space, which is no problem in two dimensions.

To display the vertices of a true *three-dimensional* quasicrystal, we project them onto a plane perpendicular to a fivefold axis. Then a point in the plane represents an entire row of vertices which smears out during relaxation. In the case of rational approximants, the calculations were done in a coordinate frame parallel to the directions of periodicity. Therefore it was necessary to rotate the sample to the fivefold axis before displaying it.

A more quantitative way to obtain structural characterization is the radial pair distribution function $G(r)$, or its Fourier transform, the powder structure factor $S(q)$:

$$S(q) = 1 + \int_0^\infty 4\pi r^2 [\rho(r) - \rho_0] \frac{\sin(qr)}{qr} dr + \int_0^\infty 4\pi r^2 \rho_0 \frac{\sin(qr)}{qr} dr, \quad (3)$$

where ρ_0 denotes the average density of atoms around a central atom. The second term of Eq. (3) yields the characteristic scattering intensity of the quasicrystal, whereas the third term describes the homogeneous part. The information contained in $G(r)$ allows us to locate nearest, next-nearest, and eventually higher-order neighbor separations, as well as to determine their coordination number. But it does not measure the bond-orientational order which is crucial for quasicrystals. Therefore we calculated, according to Steinhardt *et al.*,²⁴ the modulus

$$Q_l = \left[\frac{4\pi}{2l+1} \sum_{m=-l}^l |\bar{Q}_{lm}|^2 \right]^{1/2} \quad (4)$$

of the l th bond-orientational multipole moment

$$\bar{Q}_{lm} = \frac{1}{N_B} \sum_{\text{bond } i} Y_{lm}(\theta_i, \phi_i). \quad (5)$$

Here θ_i and ϕ_i denote polar and azimuthal angles of the i th-nearest-neighbor bond relative to a fixed laboratory coordinate system, and N_b is the number of bonds. As nearest neighbors, we defined all atoms separated a distance of less than 1.2 times the length of the first coordination shell in agreement with the definition of Ref. 24. In an isotropic medium Q_l vanishes for $l > 0$, and in hexagonal or cubic media Q_l is finite for $l=4,6,8$. In an icosahedral medium of long-range bond-orientational order Q_6 dominates, whereas Q_4 and Q_8 are zero.

Thus with Q_l we have a measure of the bond-orientational order.

For diatomic quasicrystals partial radial distribution functions and partial structure factors are defined. Although the partial distribution function is useful to determine the nearest-neighbor shells, the partial structure factors are of less use if the types of atoms are not specified exactly. We calculated $G(r)$ and $S(q)$ as if the two types of atoms were the same, and the resulting functions turned out to be typical for quasicrystalline materials. Partial bond-orientational multipole moments are not very informative because of the many differing lengths of various bond types. The numerical values do not indicate the symmetry of the sample and the changes during relaxation.

IV. TWO-DIMENSIONAL SYSTEMS

For monatomic small clusters of pentagonal symmetry, consisting, for example, of the 16 atoms of a filled decagon in the Penrose pattern, we found that they remain stable for many iterations, but finally become hexagonal. Larger clusters, for example of 30×30 atoms, quickly convert into hexagonal domains with many types of defects. These results (Fig. 1) agree essentially with those of Sasajima *et al.* in Ref. 9.

Generally, in two dimensions instability is expected for any arbitrary pattern because there is a unique crystalline packing of hard disks with isotropic potentials, which is the hexagonal one. The special reason for instability of the Penrose pattern is the anisotropic distribution of atoms within a shell.

If the potential radius is small, many bubbles are observed, diminishing when the potential radius increases until they form single vacancies. The bubbles appear because in the case of a small potential range the initial mean separation of the atoms is too large, and the interaction is of a limited range. The quasicrystal ought to be contracted; the atoms can move only marginally during each relaxation step and the hexagonal domains which they form are very rigid.

When the potential radius is large enough there are compact hexagonal domains glued together in arbitrary

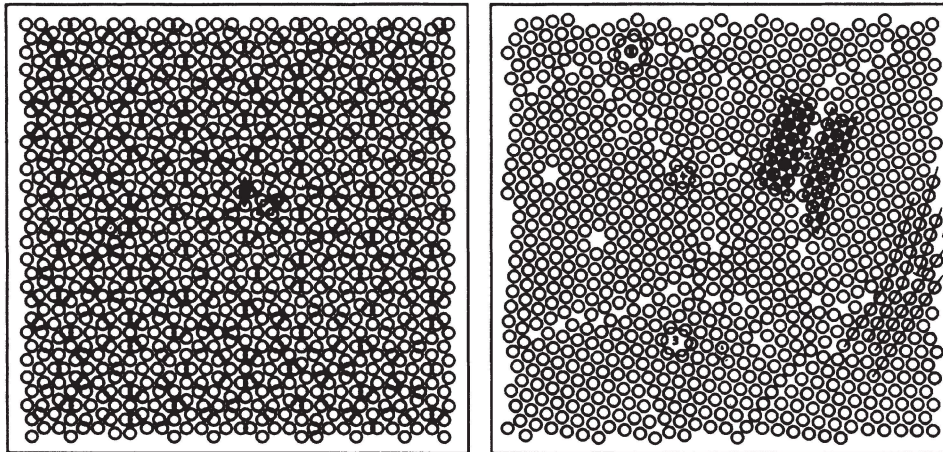


FIG. 1. Two-dimensional quasicrystal resulting from a primitive monatomic decoration of the Penrose rhombs. A large and a small rhombus are indicated. Left side, initial state; right side, final state, which contains patches of hexagonal-close-packed structure, however, with many defects like (1) dislocations, (2) grain boundaries, (3) vacancies, (4) disclinations, and (5) antidisclinations.

orientations with small-angle grain boundaries between them. Frequently atoms arrange in pentagons in the hexagonal domains, which then form the cores of disclinations. Domains of different orientations also are linked by pentagons. The counterpart of the pentagons are heptagons, quasicrystalline vertex figures with seven atoms. Heptagonal configurations are usually the centers of antidisclinations. They are always combined with other defects like dislocations and disclinations. Finally, the lattice lines are often distorted and disrupted due to the high density of defects.

For diatomic quasicrystals the decoration introduced by Lançon *et al.*⁷ and also applied by Widom¹⁰ was used. If the radii of the pair potential are optimized before relaxation, the system displays extreme stability inasmuch as the atoms in the bulk do not move at all. If the radii are scaled by a common factor, the quasicrystal expands or contracts without structural change. We find only small boundary effects when using open boundary conditions.

The calculations were mainly performed to test the algorithm and provide confidence for an extension to three dimensions. With the results in two dimensions we also gained insight into the influence of boundary conditions on the relaxation process.

V. THREE-DIMENSIONAL MONATOMIC SYSTEMS

In two dimensions we mainly confirmed the results of Refs. 7–10. To our knowledge no microscopic quantitative results exist in three dimensions. Therefore, we generalized our method for three dimensions and examined several decorations of quasicrystals, starting with a simple decoration of all vertices.

A. Systems with all vertices occupied

The smallest distance of atoms in a three-dimensional Penrose tiling is the short diagonal of the oblate rhombohedron, having length $d=0.563$ in units of the edge size. If *all* vertices are occupied, the width of the opti-

mized potential radius σ is about 0.58. The atoms of the next-largest separation, $d=1$ and 1.052, “feel” only a very small force. Therefore, the pattern is altered slowly during the iteration procedure. But, finally, it becomes unstable, although it takes approximately 500 relaxation steps. Increasing σ in the range between 0.58 and 1.03 drives the system very fast into a glassy state. We have examined three values for σ : the minimal distance 0.58, the most frequent distance 1.0, and an intermediate value 0.8, because for $\sigma=0.8$, the atoms at $d=0.563$ feel no significant repulsive force yet, but those at 1.0 are still within the attractive range of the potential.

The results are documented by our analytic tools.

1. Projection

In projection along a fivefold axis (Fig. 2) the atoms are lined up in rows. During relaxation, the alignment is lost, and the projected atoms cover the projection plane rather homogeneously (Fig. 2). If σ is small, bubbles appear like those in two dimensions, but they are not as distinctly visible as there because of the three-dimensional projection. For larger σ the situation also is like that in two dimensions: a bond length similar to the mean atomic distance forces the bubbles to vanish in the final state.

It is interesting to note that in the course of the decay the quasicrystalline phase does not pass directly into the amorphous state but via a sequence of transient states, of which we do not yet know whether their structure is similar to that of an icosahedral glass or whether they comprise a new type of icosahedral structure. In the first relaxation steps the atoms arrange in planes, which in the projection along a fivefold axis constitutes a generalized pentagonal grid with two spacings of ratio $1:\tau$ (“Amman²⁵ grid,” Fig. 3). The polygons formed by the intersecting planes are golden triangles with edge length $1,1,\tau$ or $\tau,\tau,1$. In the following steps new planes of reduced density form in between the old ones, leading to a deflated Amman grid which is scaled down by τ . The golden triangles are successively subdivided into smaller

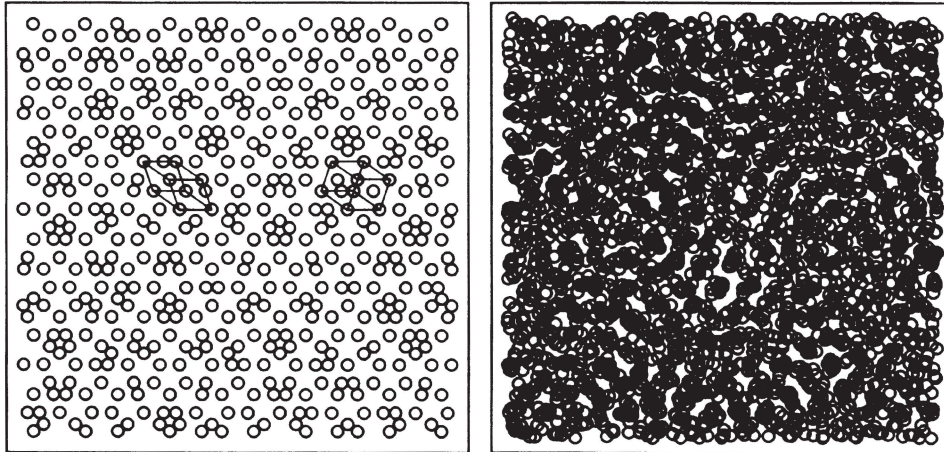


FIG. 2. Three-dimensional quasicrystal resulting from a primitive monatomic decoration. The quasicrystal is projected along the fivefold axis, and hence in the initial state each open circle represents a row of atoms lying along the projection axis. Two representative rhombohedra have been drawn. Left side, initial state, right side, final state. The amorphous character of the sample is seen clearly.

ones of similar shape. Amorphization begins when the edge length of the triangles reaches the average separation of the atoms.

This behavior reveals the hierarchy of local atomic arrangements. Those atoms which have the most anisotropic environments in the initial pattern move first, because these atoms feel the largest force. On the other hand, there are many vertices which are surrounded by 20 prolate rhombohedra, forming a neighborhood of *perfect* icosahedral symmetry. These vertices become the intersections of five Amman planes in the course of the relaxation. The central atom and its first neighbors feel no force and thus remain fixed until the last stage of amorphization.

For the pair potentials applied in this work, these intermediate structures are unstable. Thus their physical significance is unclear to us. However, using a purely repulsive potential we found that they can be stabilized. Further investigations are in progress.

2. Radial distribution function (RDF) and structure factor (SF)

Perfect quasicrystals have discrete peaks in the radial distribution function. The coordination numbers are nonintegers due to averaging over all possible vertex environments (Fig. 4). Depending on the value of σ , the *relaxed* crystal shows three or more coordination shells, but the RDF smooths off at larger separations as for a

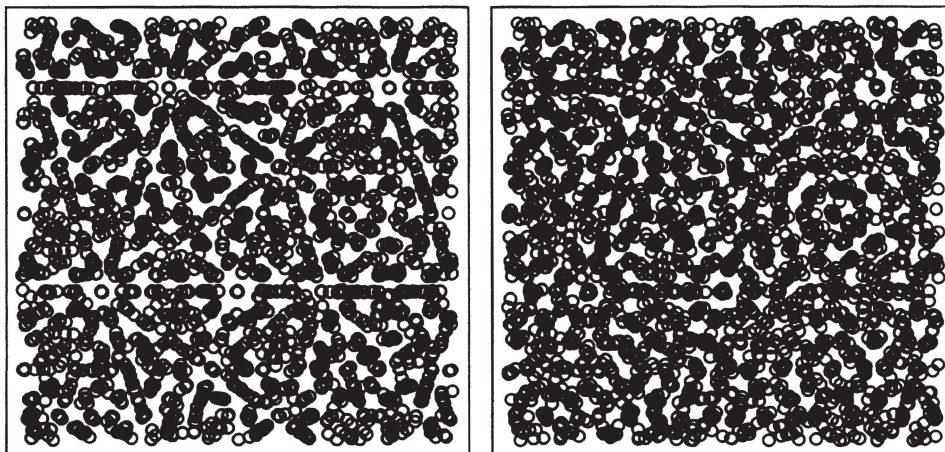


FIG. 3. Three-dimensional quasicrystal with the monatomic primitive decoration. Left side, projection after 400 iteration steps. Atoms have aligned in clearly visible Fibonacci planes. The intersection points of the Fibonacci planes are the vertices with perfect icosahedral symmetry; right side, the same quasicrystal after 800 iteration steps. The Fibonacci structure has decayed almost completely and the vertices with perfect icosahedral symmetry also begin to vanish.

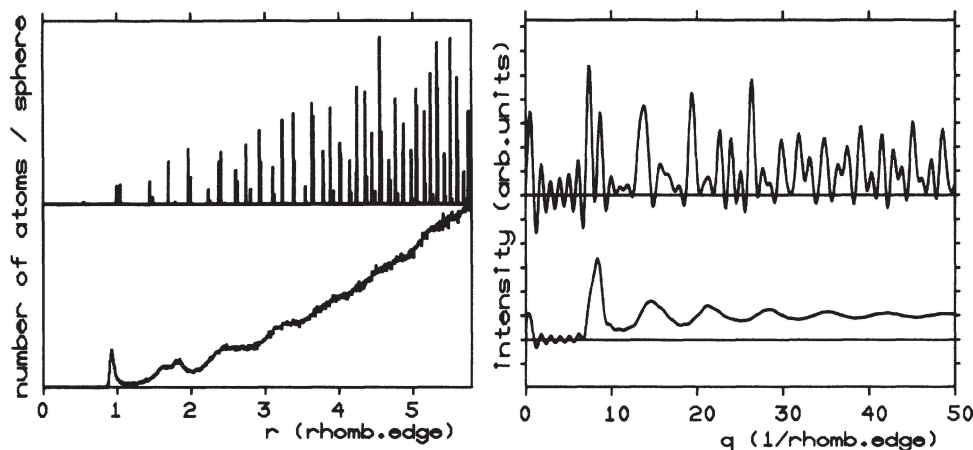


FIG. 4. Left side, radial distribution functions of the initial quasicrystalline state with the primitive monatomic decoration (upper part) and of the final amorphous state (lower part). A perfect quasicrystal has discrete peaks (like a crystal), whereas an amorphous structure only shows the peaks of the short-range order; right side, structure factor of the initial state (upper part) and the final state (lower part). Although the structure factor of an infinite quasicrystal has discrete peaks, the Fourier transform of the radial distribution function contains broad peaks and artificial fluctuations due to the finite size of our samples. In the amorphous state most of the quasicrystalline peaks have disappeared and only the short-range order remains represented by the first maximum.

homogeneous, amorphous medium.

In the initial state, there is a small coordination shell at 0.563 with a frequency of 0.76, but the most pronounced coordination shells are at 1.0 and 1.051 with frequencies of 6.00 and 6.47. The value 1.051 belongs to the short diagonal of a rhombic surface element. Thus at about 1.03, a double shell is located with an intensity of 12.47 like in dense packings. After relaxation, the initial radius of the first coordination shell is always equal to the optimal σ . The closer σ is to R , the radius of the first coordination shell of the initial configuration, the fewer steps are necessary to move the atoms from R to a new shell at σ . During relaxation, the first peak increases up to a maximum coordination number of about 10. Independent of the choice of σ , there are two further peaks at about 1.7σ and 2σ , resulting from the diagonal of two triangles sharing one side and from three atoms lying on a straight line, respectively. This split second-nearest-neighbor peak is characteristic for metallic glasses. When σ is about 1.0 further peaks exist with decreasing intensity due to the dense packing of atoms. (Note that the potential range β is coupled to the potential radius σ .) When σ is 0.8 or 0.6, there are far fewer peaks which shows that the atoms are not packed densely and that there must be vacancies and bubbles in the quasicrystal.

The powder structure factor of the perfect system (Fig. 4) displays peaks which can be identified with and indexed as those obtained by projection from six-dimensional reciprocal space. The width of the peaks, however, is finite, because in the integral [Eq. (3)] we have cut off the radial distribution function at the radius of that sphere, which just fits into the periodicity cell of the approximant of the Penrose pattern. The cutoff is also responsible for the negative value of the structure factor and the remaining oscillations at low wavelengths, which are subtracted incompletely with the term $4\pi r^2 \rho_0$ in the integral [Eq. (3)]. Otherwise, the intensity of the homo-

geneous scattering would have concealed that of the quasicrystalline scattering in which we are interested.

After relaxation, the quasicrystalline dominant peaks disappear. Only the typical structure factor of an amorphous material remains with short-wavelength modulation due to the finite range of integration.

3. Bond-orientational order

In the perfect state Q_2 , Q_4 , and Q_8 vanish as expected, but Q_6 takes the value 0.153, indicating long-range icosahedral bond orientation. The reduction of Q_6 to 2.9×10^{-2} in the course of relaxation indicates that the long-range bond order has vanished. But it does not mean that the icosahedral ordering of the nearest neighbors, which is typical in dense-packed amorphous materials, has vanished, too. To examine the short-range order one would have to calculate correlation functions and not only multipole moments.

B. Monatomic unit-sphere packing

The smallest atomic distance of 0.563 turns out to be the reason for the instability of the fully covered primitive Penrose lattice. The atoms separated by this distance form rings of ten members in the shape of a crown or chains being fractions thereof. If a chain has an even number of links, then we remove every second atom in order to leave the greatest possible number of atoms in the cluster. If a chain has an odd number of links, and in the case of rings, we also removed every second atom then beginning at an arbitrary atom. With this construction none of the remaining atoms is separated by less than 1.0 from a neighbor. There are also other constructions providing a packing with the same properties by Henley,²⁰ by Olami and Alexander,²⁶ and by Oguey and Duneau.²⁷

1. Projection

The number of removed atoms is only about 5% (Fig. 5). The structure of the projected pattern remains pentagonal. Now in the course of relaxation the structure changes by minor local fluctuations only, and the structure remains stable (Fig. 5). A more systematic algorithm for the removal of atoms would place only a fraction of the 5% of atoms involved into energetically almost equivalent positions. This could enhance the stability marginally, but is not expected to alter our results.

2. Radial distribution function and structure factor

The structure of the RDF is not changed by removing a subset of atoms; only the peak at 0.563 has vanished. During relaxation some very close peaks in the RDF (Fig. 6) merge into one; altogether the peaks stay distinct. The coordination number remains nearly unchanged and is 10.67.

The peaks of the structure factor (Fig. 6) retain their position; only the intensity is altered slightly. Local distortions cannot be identified since the peak width is finite due to the periodic boundary condition. Since the width scales like l^{-1} where l is the diameter of the periodicity cell, we expect that an infinite system shows Bragg peaks and that the long-range positional order is not disturbed in the relaxation process.

3. Bond-orientational order

The bond-order parameter Q_6 increases slightly from 0.180 to 0.183, indicating only minor changes of the icosahedral bond angles, while Q_2 , Q_4 , Q_8 are approximately zero before and after relaxation.

4. Discussion of the stability

To investigate the degree of metastability we compared the energy per atom of the quasicrystalline unit-sphere

packing with that of a bcc and fcc packing using the same potential type, the same potential radius, and the same potential range. We found an energy of -2.8 for bcc and -3.2 for fcc (both without relaxation) whereas the energy of the relaxed quasicrystalline state with periodic boundary conditions is about -2.9 and was decreased only by 1% during relaxation. This fact shows that our quasicrystalline packing can be as stable as crystalline packings.

The Landau theory up to the third order in $\rho(r)$ used in Ref. 2 leads to a similar result, i.e., the energy of the quasicrystal is below that of the bcc lattice. However, this agreement may be accidental, because Biham *et al.*⁵ have shown that this is no longer true if the fourth-order term is also taken into account (see footnote in Ref. 5).

Very recently, Olami and Alexander²⁶ have investigated the density of several packings in more detail. From their results one cannot conclude that Henley's unit-sphere packing is the densest one. But it is at least the densest known until the present.

Control calculations have been performed also with finite samples of the unit-sphere packing monatomic quasicrystal and open boundary condition. For 1888-, 6070-, and 13 189-atom clusters the energy per atom was -2.52 , -2.61 , and -2.65 , respectively, the last two configurations not having been relaxed fully. These values converge towards the energy per atom -2.86 of the sample with 1902 atoms and periodic boundary conditions (being the rational approximant 5/3). The higher energy of the open clusters is due to the surface effects. For all cases the structure in the interior of the samples was the same. Thus we may conclude that periodic boundary conditions actually simulate the behavior of samples of infinite size.

C. The stable decoration with noise

Having discovered a stable monatomic quasicrystal, it appeared to us of considerable interest to find a measure

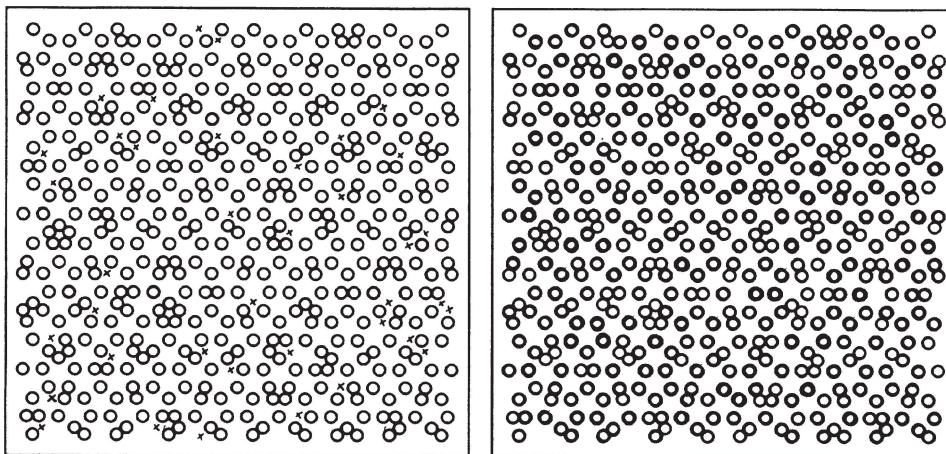


FIG. 5. Three-dimensional quasicrystal with the unit-sphere packing. The places where atoms have been taken out of the quasicrystal with the monatomic primitive decoration are marked with a cross. The quasicrystalline character of the sample has not changed. Left side, initial state; right side, final state. Only minor fluctuations appear, caused by movements of the atoms to improve their local potential energy.

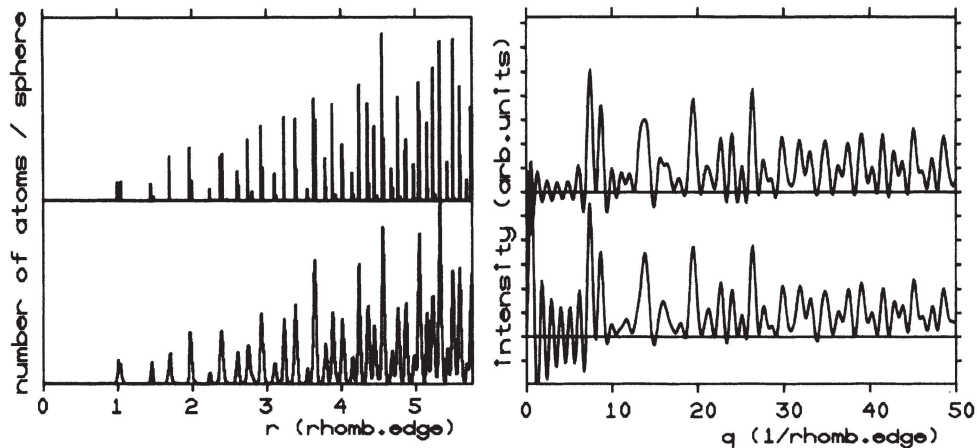


FIG. 6. Left side, radial distribution function of the unit-sphere packing. The upper part exhibits the discrete peaks of a perfect quasicrystal. The first small peak at 0.53 has disappeared. After relaxation (lower part) the peaks are broadened due to minor fluctuations, but they remain discrete; right side, structure factor. The diagrams for the initial state (upper part) and the final state (lower part) demonstrate that the quasicrystalline long-range order is unaltered and similar to that of the primitive decoration.

for the width of the metastable valley of the monatomic unit-sphere decoration. Therefore we displaced the atoms of the unit-sphere packing randomly before relaxation. The bond-orientational displacement was chosen isotropically, whereas for the radial displacement we used a Gaussian distribution. If the average displacement is increased to about 6% of the unit edge length, we note the following properties of the initial state: There is so much noise that the quasicrystalline structure has nearly vanished in the projection (Fig. 7). The RDF (Fig. 8) has lost its isolated peaks although there remain certain distinct shells and the structure appears not completely amorphous. In the structure factor (Fig. 8) the quasicrystalline peaks are small and peaks greater than 30 reciprocal edge lengths cannot be seen due to the Debye-Waller factor produced by the noise.

If the average displacement is less than 6%, then in the course of the relaxation pentagonal symmetry returns

with remarkable clarity (Fig. 7). The RDF (Fig. 8) now has small discrete peaks whereas the coordination number remains constant. The quasicrystalline peaks in the structure factor (Fig. 8) have acquired the height of the perfect quasicrystalline ones, and the peaks greater than 30 wavelengths are seen again. During relaxation, the icosahedral order *increases* slightly and the energy per atom is lowered again from -2.5 to -2.85 . The original pattern is restored completely.

But if the average displacement is chosen to be greater than 7% of the unit length, the final state is amorphous, although the initial state does not differ extremely from the case of smaller displacements (Fig. 9). If we look for the maximal displacement of the atoms in the initial state we find some which are displaced by 40% of the unit edge length and hence penetrate deep into the repulsive range of other atoms. The energy per atom is only about -1.4 and the icosahedral parameter Q_6 is changed from

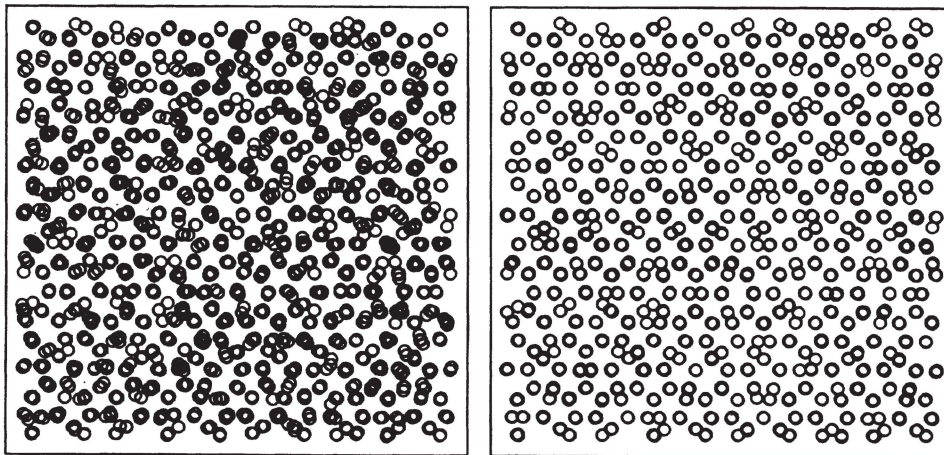


FIG. 7. Unit-sphere packing at low temperature (small noise, 6%). Atoms which have been lined up in the perfect quasicrystal are now displaced individually. Left side, initial state with fluctuations caused by the random displacements; right side, final state, where the fluctuations have disappeared and the atoms have returned to the position in the perfect state.

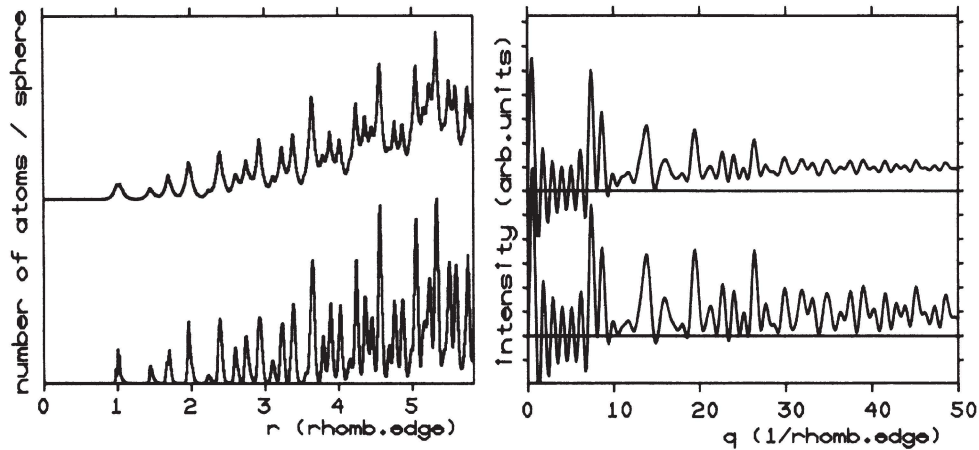


FIG. 8. Left side, radial distribution function of the unit-sphere packing with small noise. Before relaxation (upper part) the peaks are smeared out due to the displacements of the atoms, but after relaxation (lower part) the peaks are discrete like those in the RDF of the relaxed unit-sphere packing without noise; right side, structure factor. In the initial state (upper part) the quasicrystalline peaks are diminished and have nearly disappeared at higher wavelengths. After relaxation (lower part) they are as high as in the perfect quasicrystal.

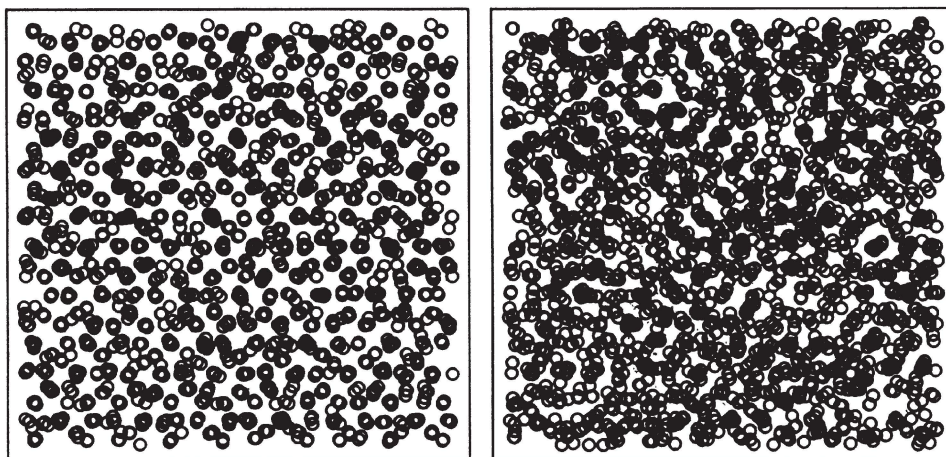


FIG. 9. Unit-sphere packing at higher temperature (large noise, 8%). Left side, initial state; right side, final state. Although the initial state is not very different from that of the quasicrystal with small noise, the structure has been changed completely into an amorphous state.

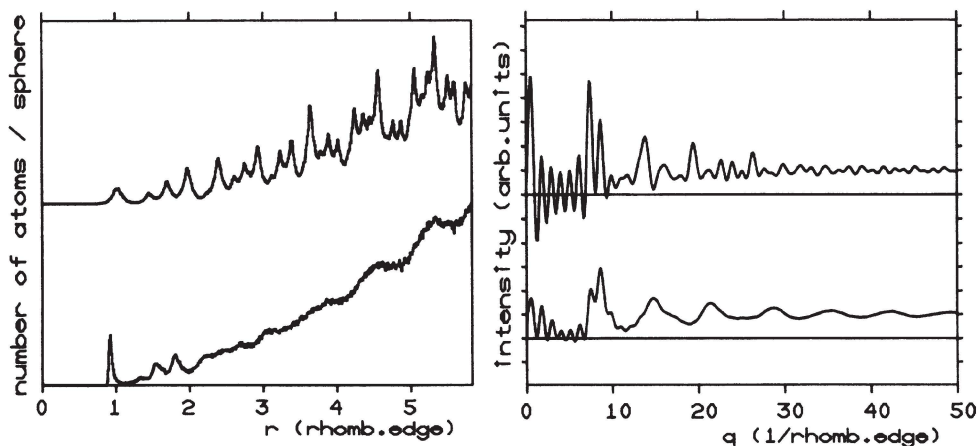


FIG. 10. Left side, radial distribution function of the unit-sphere packing with large noise. The shells of the initial state (upper part) have disappeared. The final state (lower part) is amorphous; right side, structure factor of both states. The quasicrystalline character disappears.

0.17 to 0.11. The amorphous character of the final state is revealed by the RDF (Fig. 10) as well as by the structure factor (Fig. 10). The energy per atom decreases during relaxation to -2.3 but remains higher than that of the stable phase. The icosahedral order has disappeared.

These results show that the "basin of attraction" of the metastable icosahedral configurations has a *finite* measure. Therefore it is not unlikely that a liquidlike initial configuration relaxes to a quasicrystalline structure, which would not be possible if the final state is in a "golf hole."

The basin of attraction is even larger than estimated from the maximum amplitude ϵ of the noise. This is because the noise was introduced to the initial "nonequilibrium" configuration. Nevertheless, let us assume that the relaxed quasicrystalline structure is stable against fluctuations smaller or equal to ϵ . Taking as elastic constant E/σ^2 we can determine a lower bound for the barrier separating the relaxed configuration from any other locally stable configuration to be of the order of $\Delta E_{\min} = E(\epsilon/\sigma)^2$. Thus for temperatures for which kT is much smaller than ΔE_{\min} the lifetime of the relaxed structure may become very large.

The results do not prove that real monatomic quasicrystals must exist, but for their existence these properties are necessary.

VI. THREE-DIMENSIONAL DIATOMIC SYSTEMS

Until now, monatomic quasicrystals have not been discovered as well as monatomic metallic glasses. For the latter this is due to the fact that the cooling rates available today are too low. For the presently largest cooling rates of about 10^8 K/sec the monatomic metals still crystallize. From computer simulations it is estimated that cooling rates of 10^{13} K/sec were required.²⁸ For intermediate rates a structure between crystalline and amorphous may occur. Whether or not this structure is quasicrystalline cannot be answered. It would be interesting to perform molecular-dynamics simulations with variable cooling rates.

We therefore investigated also diatomic quasicrystals with respect to stability.

There are many possibilities to decorate a quasilattice. We studied decorations which have been proposed for aluminum-based icosahedral phases.

We will use two decorations derived by Henley and Elser^{22,29,30} from periodic alloys. They involve the Mackay icosahedra (MI) and the truncated icosahedra (TI), also examined by Guyot and Audier in Refs. 31–33. The decorations were slightly modified following Dubois and Fruchart in Refs. 34 and 35.

The parameters to be fitted are now the bond lengths σ_{ab} , the potential ranges β_{ab} , and the bonding strengths (bond energies) E_{ab} between atoms of types a and b . In all cases we used optimized bond lengths and $\beta_{ab} = 2\sigma_{ab}$. In molecular-dynamics and Monte Carlo simulation studies (Refs. 7, 9, and 10) it is necessary to choose the bond strength between different atoms to be greater than between equal atoms to avoid phase separations, and thus often $E_{12} = 2E_{11} = 2E_{22}$ is used. In our model the atoms

have very low mobility, and therefore phase separations are almost impossible. Hence arbitrary values for E_{ab} can be taken, but this option was not examined here when the system was stable. We used the same relations as in Refs. 7, 9, and 10. Only in the case of unstable decorations have we also chosen other relations between the bond strengths, but stability was not dependent on the specific set of bond strengths. Only the shape of the peak of nearest-neighbor atoms in the radial distribution function varied slightly.

A. Mackay icosahedra

1. Description of the decoration

In the decoration related to the MI model (Fig. 11) six atoms of the first type are placed on the vertices of a prolate rhombohedron. The acute corners are left empty. Six atoms of the second type are placed at the center of the edges near the acute corners and six at the points dividing the long diagonal of the rhombic surface elements in the ratio $\tau:1$.

Once the prolate rhombohedra are filled with atoms, then also the decoration of the oblate rhombohedron is fixed. This simple form of decoration, however, turned out to be very unstable and therefore was modified.

There are two atoms of short separation in the oblate rhombohedron, namely those lying on a front and a back face of the solid. From each pair we removed one partner. There are also short bonds between atoms from the edges and on the faces, together with voids in other parts of the rhombohedron. We have removed the atoms on the edges of the oblate rhombohedron, thereby also changing the decoration of the prolate rhombohedra. By this procedure the bond lengths are modified and binding energy is increased, but the stability of the decoration is not improved.

2. Results

The results of the relaxation are similar to those obtained from the monatomic decoration with all vertices

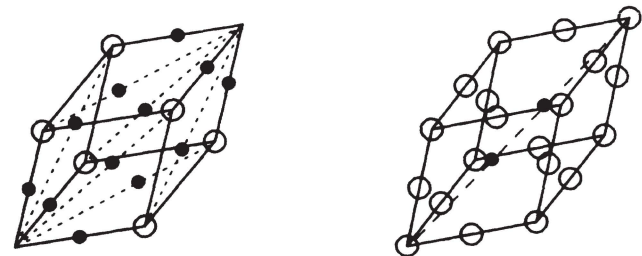


FIG. 11. The prolate rhombohedron in the diatomic decorations. Left side, MI decoration; right side, TI decoration. The two types of atoms are drawn in different sizes. In the MI decoration the rhombic diagonals are divided in the ratio $\tau:1$. In the TI decoration the major diagonal of the rhombohedron is divided in the ratios $\tau:1:\tau$. The decoration of the oblate rhombohedron follows from the common rhombs.

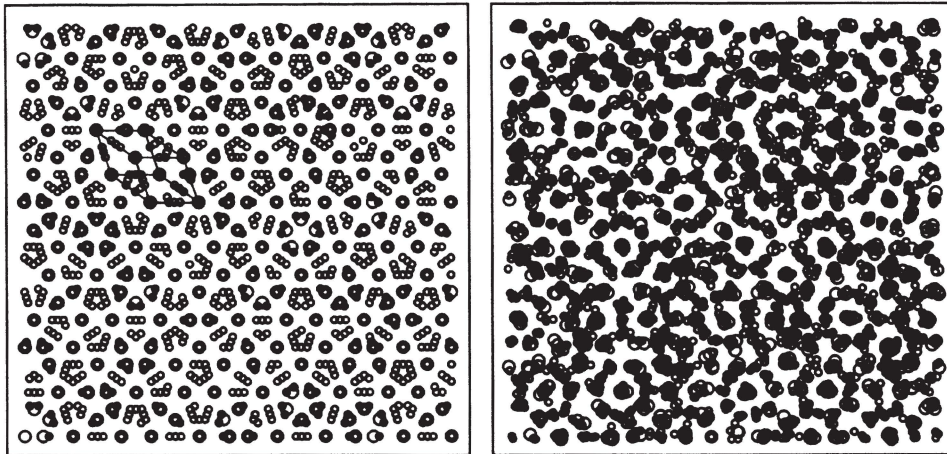


FIG. 12. MI decoration, one prolate rhombohedron has been drawn. As in Fig. 11, different sizes of rings denote different types of atoms. Left side, initial state; right side, final state. The initial order has decayed and the final state is amorphous. At the vertices with perfect icosahedral symmetry, the structure seems to be more stable.

occupied: In the projection we see that the quasicrystal-line structure vanishes although the final state does not seem to be completely amorphous (Fig. 12). The relaxation is very slow; highly symmetrical vertices and their environment remain fixed for many iterations. But the radial distribution function (Fig. 13) is typical for an amorphous material and so is the structure factor (Fig. 13). The energy of the quasicrystal, which has been only -1.02 , decreases to -1.36 in the case of the original decoration and from -1.46 to -1.84 in the case of the modified one.

The reason for instability may be that the MI decoration does not yield a dense packing of two types of spheres for the oblate rhombohedron. The atoms move from their initial positions into the voids.

B. Truncated icosahedra

1. Description of the decoration

The second type of decoration considered is related to the TI model. One sort of atom is placed at the vertices

and on the middle of all edges. These surround vacancies in the form of cages with centers on the principal diagonal at $\tau:1:\tau$. They are filled with atoms of the second type (Fig. 11). The decoration of the oblate rhombohedron is again determined by the adjoining prolate rhombohedra, but now comprises a very dense packing of two types of spheres, and we expect stability.

2. Results

A quasicrystal with the TI decoration remains stable as seen by comparing the initial and the final state in Fig. 14. The radial distribution function (Fig. 15) and the structure factor (Fig. 15) emphasize this conclusion. There are only small fluctuations of the atoms around their initial positions. The peaks in the radial distribution function are broadened slightly and the intensity of the structure factor decreases by only a small amount. The energy is lowered from -2.35 to -2.37 .

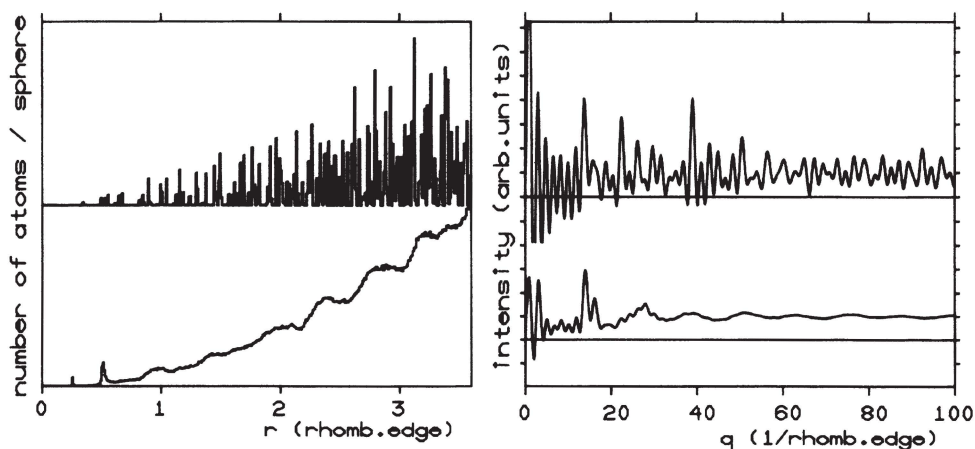


FIG. 13. Left side, radial distribution function of the MI decoration. The two different types of atoms are not distinguished, but the changes from the initial state (upper part) to the final state (lower part) can be immediately seen; right side, structure factor. The types of atoms are not distinguished, also.

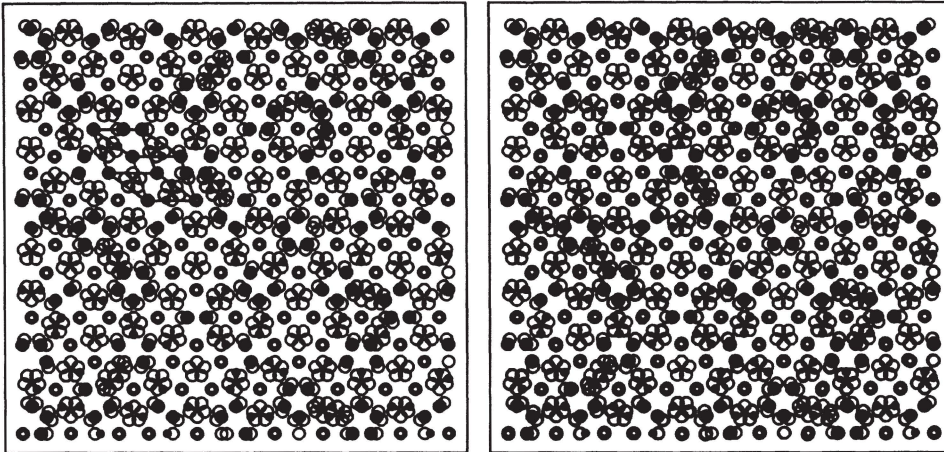


FIG. 14. TI decoration, one prolate rhombohedron has been drawn. The different types of atoms are indicated by different sizes of rings as in Fig. 11. Left side, initial state; right side, final state. As can be seen from the discrete character of the picture, the structure is unaltered during relaxation.

C. Truncated icosahedra with noise

Also, for the stable diatomic decoration we investigated the degree of metastability by statistical displacement of the atoms in the initial state.

Contrary to the monatomic stable decoration, no sharp value for the mean displacement was found, which allowed us to distinguish relaxation back to an ordered state from decay to an amorphous state.

Even when the mean displacement was 25% of the edge length (which corresponds to about 50% of some atomic separations), and although the RDF and SF were completely smeared out, after a sufficient number of iteration steps (about 3000 or 4000) the order returned, to our surprise, and the potential energy of the relaxed state was nearly independent of the degree of displacement. The characteristic peaks of the relaxed perfect quasicrystal can be seen in the RDF and SF, whereas in the projec-

tion a rest of disorder is found.

Although the phenomenon is not yet understood completely, we suggest two possible interpretations: (i) the truncated-icosahedron decoration represents a so-called tetrahedrally close-packed (tcp) structure (Refs. 13 and 36), where all atoms arrange in almost perfect tetrahedra. When the random displacements are applied some tetrahedra are destroyed so that the quasicrystal contains voids and interstitials. In the course of the relaxation new tetrahedra may be formed, and thus the coordination number (and therefore the potential energy) returns to the value of the perfect quasicrystal. The tcp structure appears highly degenerated. (ii) Before relaxing the quasicrystal we had fitted the potential radii to the geometry of the perfect Penrose pattern. Maybe our calculations yield a hint that quasicrystalline order can *grow* out of disorder if the atomic sizes are adjusted.

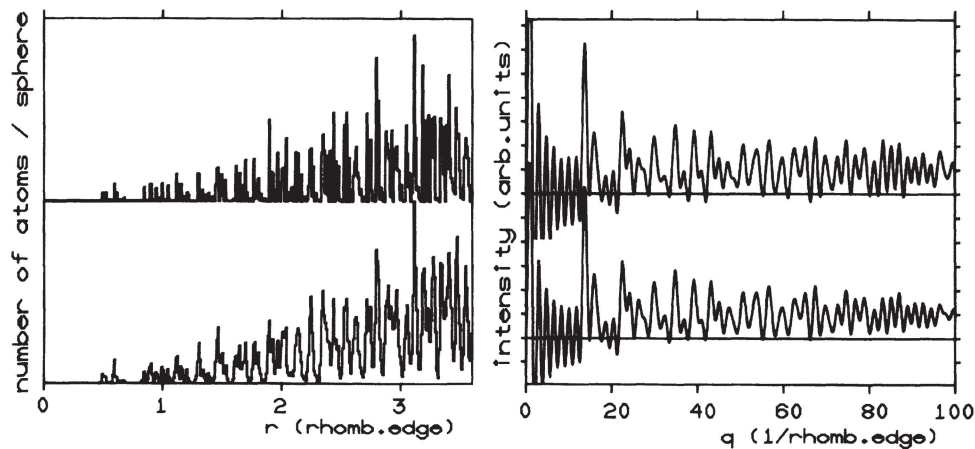


FIG. 15. Left side, radial distribution function of the TI decoration, again no distinction between the type of atoms has been made; right side, structure factor, the comparison of the initial states (upper parts) with the final state (lower part) demonstrates the stability of this decoration.

VII. SUMMARY AND DISCUSSION

We have simulated the relaxation of quasicrystalline structures by the method of steepest descent. In two dimensions, results obtained with the molecular-dynamics method were confirmed. The monatomic quasicrystals are unstable because there is an optimal packing for identical spheres. However, diatomic quasicrystals in two dimensions with the decoration of Lançon *et al.*^{7,8} are stable. Extending the method to three dimensions, we find that a monatomic quasicrystal with all vertices occupied is unstable because certain atoms with very short separations disturb a unit-sphere packing. If one partner of these pairs is removed, a stable decoration is obtained, not only at 0 K, but also at higher temperatures. Thus within the limitations of our model *monatomic* quasicrystals can really exist. After examining diatomic quasicrystals we can state that decorations related to the Mackay icosahedra are unstable, whereas the truncated-icosahedron decoration is stable.

During our calculations we found more and more that the crucial criterion of stability of a quasicrystalline decoration is the density of the packing of one or two

types of spheres. This fact can be understood by recalling the properties of the potential we have used: the Lennard-Jones potential is isotropic. Therefore it does not prefer any bond-orientational symmetry. It favors dense packings of spheres, because the denser a packing is the more bonds per atom exist and the larger the binding energy per atom becomes.

Very recently Elswijk *et al.*³⁷ determined the structure of quasicrystals of the Al-Cu-Li type experimentally and found that they can be described exactly with the TI decoration involving a random distribution of Al and Cu atoms on the edges and vertices of the rhombohedra. We therefore conclude that our calculations do not only describe a rather artificial decoration but a realistic one and can also contribute to the experimental discussion of the structure of quasicrystals.

ACKNOWLEDGMENTS

One of us (R.S.) would like to thank the Institut für Theoretische und Angewandte Physik (Stuttgart), where this work was started, for its hospitality.

- ¹M. V. Jarić, Phys. Rev. Lett. **55**, 607 (1985).
²P. A. Kalugin, A. Y. Kitaev, and L. S. Levitov, J. Phys. (Paris) Lett. **46**, L601 (1985); Pis'ma Zh. Eksp. Teor. Fiz. **41**, 119 (1985) [JETP Lett. **41**, 145 (1985)].
³N. D. Mermin and S. M. Troian, Phys. Rev. Lett. **54**, 1524 (1985).
⁴P. Bak, Phys. Rev. Lett. **54**, 1517 (1985).
⁵O. Biham, D. Mukamel, and S. Striktman, Phys. Rev. Lett. **56**, 2191 (1986).
⁶B. Chakraborty, Phys. Rev. B **34**, 8202 (1986).
⁷F. Lançon, L. Billard, and P. Chaudhari, Europhys. Lett. **2**, 625 (1986).
⁸F. Lançon and L. Billard, J. Phys. (Paris) **49**, 249 (1988).
⁹Y. Sasajima, T. Miura, M. Ichimura, M. Imabayashi, and R. Yamamoto, J. Phys. F **17**, L53 (1987).
¹⁰M. Widom, K. J. Strandburg, and R. H. Swendsen, Phys. Rev. Lett. **58**, 706 (1987).
¹¹P. W. Leung, C. L. Henley, and G. V. Chester, Phys. Rev. B **39**, 446 (1989).
¹²T. Janssen, in *Quasicrystalline Materials, Proceedings of the Institut Max von Laue-Paul Langevin/CODEST Workshop, Grenoble*, edited by Ch. Janot and J. M. Dubois (World Scientific, Singapore, 1988), p. 327.
¹³K. Y. Szeto and J. Villain, Phys. Rev. B **36**, 4715 (1987); notice also the comment by D. P. Shoemaker and C. B. Shoemaker in Phys. Rev. B **38**, 6319 (1988).
¹⁴S. E. Burkov and L. S. Levitov, Europhys. Lett. **6**, 233 (1988).
¹⁵S. Narasimhan and M. V. Jarić, Phys. Rev. Lett. **62**, 454 (1989).
¹⁶D. Levine and P. J. Steinhardt, Phys. Rev. B **34**, 596 (1986).
¹⁷J. E. S. Socolar and P. J. Steinhardt, Phys. Rev. B **34**, 617 (1986).
¹⁸A. Katz, Commun. Math. Phys. **118**, 263 (1988).
¹⁹J. Roth, J. Bohsung, R. Schilling, and H.-R. Trebin, in *Quasicrystalline Materials, Proceedings of the Institut Max von Laue-Paul Langevin/CODEST Workshop, Grenoble*, edited by Ch. Janot and J. M. Dubois (World Scientific, Singapore, 1988), p. 65.
²⁰C. L. Henley, Phys. Rev. B **34**, 797 (1986).
²¹D. Gratias and J. W. Cahn, Scr. Metall. **20**, 1193 (1986).
²²V. Elser and C. L. Henley, Phys. Rev. Lett. **55**, 2883 (1986).
²³D. Mercier and J.-C. S. Levy, Phys. Rev. B **27**, 1292 (1983).
²⁴P. J. Steinhardt, D. R. Nelson, and M. Ronchetti, Phys. Rev. B **28**, 784 (1983).
²⁵B. Grünbaum and G. L. Shepard, *Tilings and Patterns* (Freeman, New York, 1987), p. 547.
²⁶Z. Olami and S. Alexander, Phys. Rev. B **37**, 3973 (1988).
²⁷C. Oguey and M. Duneau, Europhys. Lett. **7**, 49 (1988).
²⁸M. S. Watanabe and K. Tsumuraya, J. Chem. Phys. **87**, 4891 (1987).
²⁹C. L. Henley, J. Non-Cryst. Solids **75**, 91 (1985).
³⁰C. L. Henley, Philos. Mag. B **53**, L59 (1986).
³¹M. Audier and P. Guyot, Philos. Mag. B **53**, L43 (1986).
³²M. Audier, P. Sainfort, and B. Dubost, Philos. Mag. B **54**, L105 (1986).
³³P. Guyot and M. Audier, Philos. Mag. B **52**, L15 (1985).
³⁴R. Fruchart and J. M. Dubois, C. R. Acad. Sci. Paris Ser. II, **305**, 661 (1987).
³⁵R. Fruchart, J. M. Dubois, C. R. Acad. Sci. Paris Ser. II, **305**, 1413 (1987).
³⁶D. R. Nelson, Phys. Rev. B **28**, 5515 (1983).
³⁷H. B. Elswijk, J. Th. M. De Hosson, S. van Smaalen, and J. L. de Boer, Phys. Rev. B **38**, 1681 (1988).